Systems/Circuits

Deletion of the Clock Gene *Bmal2* Leads to Alterations in Hypothalamic Clocks, Circadian Regulation of Feeding, and Energy Balance

Rosana Dantas-Ferreira,[1] Dominique Ciocca,[2] Patrick Vuillez,[1] Stéphanie Dumont,[1] Christian Boitard,[3] Ute C. Rogner,[3] and Etienne Challet[1]

[1]Institute of Cellular and Integrative Neurosciences, Centre National de la Recherche Scientifique (CNRS), University of Strasbourg, Strasbourg 67000, France, [2]Chronobiotron, CNRS, University of Strasbourg, Strasbourg 67000, France, and [3]Institut Cochin, CNRS, Institut National de la Santé et la Recherche Médicale (INSERM), Université Paris Cité, Paris 75014, France

BMAL2 (ARNTL2) is a paralog of BMAL1 that can form heterodimers with the other circadian factors CLOCK and NPAS2 to activate transcription of clock and clock-controlled genes. To assess a possible role of *Bmal2* in the circadian regulation of metabolism, we investigated daily variations of energy metabolism, feeding behavior, and locomotor behavior, as well as ability to anticipate restricted food access in male mice knock-out for *Bmal2* (B2KO). While their amount of food intake and locomotor activity were normal compared with wild-type mice, B2KO mice displayed increased adiposity (1.5-fold higher) and fasted hyperinsulinemia (fourfold higher) and tended to have lower energy expenditure at night. Impairment of the master clock in the suprachiasmatic nuclei was evidenced by the shorter free-running period (−14 min/cycle) of B2KO mice compared with wild-type controls and by a loss of daily rhythmicity in expression of intracellular metabolic regulators (e.g., *Lipoprotein lipase* and *Uncoupling protein 2*). The circadian window of eating was longer in B2KO mice. The circadian patterns of food intake and meal numbers were bimodal in control mice but not in B2KO mice. In response to restricted feeding, food-anticipatory activity was almost prevented in B2KO mice, suggesting altered food clock that controls anticipation of food availability. In the mediobasal hypothalamus of B2KO mice, expression of genes coding orexigenic neuropeptides (including *Neuropeptide y* and *Agouti-Related Peptide*) was downregulated, while *Lipoprotein lipase* expression lost its rhythmicity. Together, these data highlight that BMAL2 has major impacts on brain regulation of metabolic rhythms, sleep–wake cycle, and food anticipation.

Key words: **circadian rhythm; clock genes; energy expenditure; food intake; meal anticipation; obesity**

Significance Statement

Circadian misalignment is now recognized as a condition triggering metabolic disorders. Using a combination of behavioral, physiological, and molecular approaches in the hypothalamus, we report here that ablation of *Bmal2* impairs function of hypothalamic clocks, modifies temporal distribution of food intake and energy expenditure, and leads to increased adiposity. These findings highlight that close interactions between circadian rhythmicity and metabolic pathways are dysfunctional in the absence of *Bmal2* and reveal that the transcription factor BMAL2 plays a role in the brain regulation of circadian clocks and energy metabolism. Accordingly, this work provides new evidence that altered circadian rhythmicity can be involved in the etiology of metabolic diseases.

Received Oct. 16, 2023; revised Feb. 2, 2024; accepted Feb. 8, 2024.

Author contributions: U.C.R. and E.C. designed research; R.D.-F., P.V., S.D., and E.C. performed research; D.C., C.B., and U.C.R. contributed unpublished reagents/analytic tools; R.D.-F., P.V., S.D., and E.C. analyzed data; R.D. wrote the paper.

We thank GenomEast platform (IGBMC, Illkirch, University of Strasbourg, France) for qPCR analysis. This work was supported by recurrent grants from CNRS, INSERM, University of Strasbourg (UPR3212 CNRS), and Université Paris Cité (U1016 INSERM).

The authors declare no competing financial interests.

Correspondence should be addressed to Ute C. Rogner at ute.rogner@inserm.fr or Etienne Challet at challet@inci-cnrs.unistra.fr.

https://doi.org/10.1523/JNEUROSCI.1886-23.2024

Introduction

The circadian system, comprising circadian clocks in the brain and peripheral organs, controls the daily variations of feeding and energy metabolism. In mammals, a master clock is located in the suprachiasmatic nuclei of the hypothalamus (SCN), while other brain regions and peripheral tissues harbor secondary clocks (i.e., circadian clocks receiving temporal cues from the master clock). Light perceived by the retina is the most potent synchronizer of the SCN clock, while feeding time can phase-shift secondary clocks (Mohawk et al., 2012). When food access

is limited every day at the same time, animals develop an anticipatory bout of activity prior to meal time that persists after SCN lesion (Mistlberger, 2011). Food-entrainable clocks driving food-anticipatory activity and reset by feeding cues define a food clock that specifically tracks timing of food availability (Challet, 2019). Altogether, the circadian multioscillatory system allows a temporal segregation across a 24 h cycle between conflicting or incompatible metabolic processes from molecular to behavioral levels. As a consequence, the daily period of wakefulness is concomitant with foraging, feeding, and replenishment of energy stores, whereas the daily period of sleep is associated with fasting and utilization of energy stores. Changes in this balance due to mistimed feeding or chronodisruption have deleterious impact on metabolic health (Scheer et al., 2009; Salgado-Delgado et al., 2010; S. Q. Shi et al., 2013; Arble et al., 2015).

The intracellular clockwork involves specific genes, called clock genes that interact with each other to generate self-sustained oscillations, with a period close to 24 h. The main positive loop includes two basic helix-loop-helix (bHLH) proteins containing PER-ARNT-SIM (PAS) domains: *Basic helix-loop-helix ARNT like 1* (BMAL1) and *Circadian locomotor output kaput* (CLOCK). BMAL1 and CLOCK dimerize to stimulate the transcription of other circadian factors such as *Period* (*Per1-3*) and *Cryptochrome* (*Cry1-2*) and clock-controlled genes via binding to E-boxes in their promoter. After being translated, PERs and CRYs dimerize and translocate to the nucleus where they repress CLOCK/BMAL1 activation of transcription until they are degraded. Such relieve of inhibition of PERs/CRYs allows a new circadian cycle to start. In addition, nuclear receptors REV-ERB(α,β) and ROR(α,β,γ) compete to modulate the transcription of *Bmal1* and *Clock* (Mohawk et al., 2012).

BMAL2 (also called ARNTL2, CLIF, or MOP9) is a paralog of BMAL1 that forms heterodimers with CLOCK and Neuronal PAS domain 2 (NPAS2) to activate transcription via E-box sequences (Hogenesch et al., 2000; Ikeda et al., 2000; Dardente et al., 2007; S. Shi et al., 2010; Olkkonen et al., 2017). As for other bHLH-PAS clock proteins, CRYs and PERs proteins also modulate transactivation and phosphorylation of BMAL2 (Dardente et al., 2007; Sasaki et al., 2009). Alternative splicing yields BMAL2 variants with variable transcriptional efficiency (Schoenhard et al., 2002; Dardente et al., 2007). Of note, *Bmal2* is markedly expressed in the brain, including the SCN clock, and many peripheral organs such as the liver, thymus, and spleen (Hogenesch et al., 2000; Ikeda et al., 2000; Okano et al., 2001; Hung et al., 2006). Constitutive expression of *Bmal2* rescues a number of circadian alterations resulting from *Bmal1* knock-out (KO), indicating that BMAL1 and BMAL2 are functionally redundant and that *Bmal2* transcription is regulated by BMAL1 (S. Shi et al., 2010). BMAL2 is involved in type 1 diabetes and the immune system, notably via control of thymocyte apoptosis (He et al., 2010a,b; Lebailly et al., 2015, 2017). *Bmal1* KO induces metabolic alterations, such as insulin resistance, increased adiposity, and arrhythmic oxygen consumption. Transgenic expression of *Bmal2* in *Bmal1* KO mice rescues regular insulin sensitivity and rhythmic oxygen consumption (S. Shi et al., 2010; S. Q. Shi et al., 2013). Moreover, genetic polymorphism of *Bmal2* in humans is associated with adiposity (Costa-Urrutia et al., 2019) or with diabetes in obese subjects (Yamaguchi et al., 2015).

Accordingly, this study aimed to determine whether BMAL2 regulates metabolic and behavioral circadian rhythms by investigating circadian variations in energy metabolism, feeding behavior, and locomotor activity in mice lacking *Bmal2*.

Materials and Methods

Animals. Three- to four-month-old male C57BL/6J mice (Pasteur Institute, Paris, France) were housed in a 12 h light/dark cycle, with times of lights on and lights off being defined by Zeitgeber Time (ZT) 0 and ZT12, respectively, at 22 ± 1°C and 55 ± 5% humidity. Food (rodent chow, SAFE Diet 105; SAFE Augy, France) and ultraviolet-treated tap water were available *ad libitum*, unless stated otherwise. Mice with mutated exon 4 of *Bmal2* (*Arntl2*) gene (noted B2KO thereafter) do not express BMAL2 (for details on genetic deletion and KO validation, see Lebailly et al., 2017). Both KO mice and wild-type (WT) controls were kept in individual transparent plastic cages for actimetry and calorimetry. Each cage was enriched with a running wheel and a piece of wood throughout the experiment, except during calorimetry.

All experiments were performed in Chronobiotron platform (UMS3415, CNRS and University of Strasbourg, France) in accordance with the National Institutes of Health (NIH; Bethesda, Maryland) *Guide for the Care and Use of Laboratory Animals* and the French National Law (implementing the European Union Directive 2010/63/EU), and they were approved by the Regional Ethical Committee of Strasbourg for Animal Experimentation (CREMEAS) and authorized by the French Ministry of Higher Education and Research (APAFIS #01031.01).

Calorimetry and feeding pattern. To determine daily patterns of energy expenditure and respiratory exchange ratio (RER), mice were transferred in individual metabolic cages using an open-circuit indirect calorimetry system (Addenfi, Les Cordeliers). This setup also recorded feeding behavior using an automated weighing system of the feeder. Mice were acclimatized to the metabolic cages during 4 consecutive days under light/dark conditions (as above). Measurements and analyses were performed after transfer to constant darkness on the fifth day. Projected times of lights on and lights off from the previous light/dark cycle were, respectively, called Circadian Time (CT) 0 and CT12. Energy expenditure and RER, defined as the ratio of produced CO_2 production and consumed O_2, were calculated using AlabSuite (version 1.55, Addenfi). This software was also used to analyze the temporal structure of feeding over 24 h, including food intake, eating bouts (i.e., contacts with the feeder associated with food intake of at least 0.05 g), number of meals (defined here as one or more eating bouts separated by at least 300 s without food intake), and meal duration (Sen et al., 2018).

Circadian rhythm of wheel-running activity. Mice fed *ad libitum* were initially exposed to light/dark conditions (as above). Then, they were transferred to constant darkness during 2 weeks to assess their free-running rhythmicity using wheel-running activity as circadian parameter. Thereafter, mice were transferred back to light/dark conditions. The free-running period in constant darkness was determined with χ^2 periodogram (ClockLab, Actimetrics).

Meal anticipation. Under light/dark cycle, WT and B2KO mice were fed *ad libitum* for 2 weeks and then exposed to restricted feeding schedules. Access to food was set automatically by the Fasting plan system (Intellibio). During the first week, food availability was progressively reduced to 6 h per day, from ZT6 to ZT12. Six-hour restricted feeding was maintained during the next 2 weeks under light/dark cycle. Thereafter, 6 h restricted feeding was given under a skeleton photoperiod (i.e., 1 h dawn light pulse from ZT0 and ZT1 and 1 h dusk light pulse from ZT11 to ZT12) for 2 weeks. This step allows evaluating possible masking effects of light on food-anticipatory activity, while keeping the master clock synchronized to light (Patton et al., 2013). Then, mice were transferred to constant darkness for 1 week, while maintaining the schedule of restricted feeding. Finally, all mice were fed *ad libitum* and kept 1 additional week in constant darkness.

Plasma metabolites and insulin. Two groups of B2KO and WT mice ($n = 8$ and $n = 7$, respectively) fed *ad libitum* under light/dark cycle were killed at ZT6 with a lethal dose of pentobarbital (200 $mg \cdot kg^{-1}$; CEVA). Food access was prevented 3 h before the experiment to avoid any acute effect of feeding cues on blood parameters. An intracardiac blood sample

was taken with 4% ethylenediaminetetra-acetic acid (EDTA, used as anticoagulant) to assay plasma metabolites and insulin after centrifugation for 10 min (4,600 × *g* at 4°C). Six groups of B2KO and WT mice were killed every 4 h ($n = 4$ per genotype) by intraperitoneal injections of lethal doses (respectively, 80 and 20 mg·kg^{-1}) of Zoletil (Virbac) and xylazine (Paxman, Virbac). Sampling of intracardiac blood as described above started at lights on (i.e., ZT0) followed by ZT4, ZT8, ZT12 (lights off), ZT16, and ZT20. Plasma glucose was determined with GOD-PAP kit (Biolabo). Concentrations of nonesterified fatty acids (NEFAs) were evaluated with NEFA-HR(2) kit (Wako Chemicals). Plasma levels of total cholesterol were measured by LP80106 kit (Biolabo). Plasma concentrations of insulin were determined by an Ultrasensitive mouse insulin ELISA kit (#90080, Crystal Chem).

RNA extraction and real-time qPCR analysis. In the B2KO and WT mice ($n = 24$ per genotype) mentioned above, the brain was sampled every 4 h, starting at ZT0. The suprachiasmatic region (SCN) of the hypothalamus was microdissected visually with a razor blade, based on rostrocaudal borders of the optic chiasma (i.e., from the end of preoptic area to retrochiasmatic level), ranging from bregma −0.2 to −0.9 mm, ±0.5 mm on each side of the midline (i.e., 1 mm width) and with a ventrodorsal height of 0.5 mm from the hypothalamic floor (Paxinos and Franklin, 2001).

The mediobasal hypothalamus (MBH, including the arcuate, the dorsomedial and ventromedial hypothalamic nuclei, and lateral hypothalamic area) was microdissected rostrocaudally from the retrochiasmatic level to the hypothalamic posterior region (i.e., from bregma −0.9 to −2.5 mm), ±1.5 mm on each side of the midline (i.e., 3 mm width), and with a ventrodorsal height of 1.5 mm from the hypothalamic floor (Paxinos and Franklin, 2001). SCN and MBH were immediately frozen in liquid nitrogen and stored at −80°C. The MBH was chosen because it contains several secondary circadian clocks (Guilding et al., 2009), and it is a crucial brain region for the regulation of food intake and energy metabolism (Berthoud et al., 2021).

Hypothalamic samples were homogenized in phenol/guanidine-based reagent, and total RNA was extracted according to the manufacturer's protocol (RNeasy Lipid Tissue Mini Kit, Qiagen France SAS). The concentration and purity of RNA were evaluated on NanoDrop ND-100 spectrophotometer (NanoDrop Technologies; A260/A280 and A260/A230 values were >1.8). Integrity of the RNA was assessed using 2100 Bioanalyzer (Agilent Technologies; RIN >7). cDNAs were synthesized from 100 ng of total RNA using the Fluidigm Reverse Transcription Master Mix (Fluidigm P/N-100-6297). A specific preamplification (STA: Specific Target Amplification) was performed in a multiplex polymerase chain reaction (PCR) using a pool of all primers in each cDNA sample and a pool of cDNA (Fluidigm P/N 100-5744). qPCR step was performed on 48.48 Dynamic Array integrated fluidic circuit (IFC; Fluidigm) by the GenomEast platform, a member of the "France Génomique" consortium (ANR-10-INBS-0009). No-template reactions were performed as negative controls for each primer pair. The PCR mix contained the internal passive reference dye 6-carboxyl-X-rhodamine (ROX) for normalization of the potential non-PCR-related fluorescence fluctuations. A dilution curve of pooled cDNA samples was used to calculate the amplification efficiency for each primer set and determine the optimal cDNA dilution according to the manufacturer's instructions. Relative expression levels were determined using the comparative ΔCT method to normalize target gene mRNA TATA box binding protein (Tbp; reference below).

The following TaqMan Gene Expression Assays (Applied Biosystems) were used:

AgRP (Mm00475829_g1)
Bmal2/Arntl2 (Mm00549497_m1)
Bmal1/Arntl1 (Mm00500226_m1)
Cartpt (Mm04210469_m1)
Ciart/Chrono (Mm01255905_g1)
Clock (Mm00455950_m1)
Cry1 (Mm00514392_m1)
Cry2 (Mm00546062_m1)
Dnm1l/Drp1 (Mm01342903_m1)
Gfap (Mm01253033_m1)
Ghsr (Mm00616415_m1)
Hcrt/Orexin (Mm01964030_s1)
Hdc (Mm00456104_m1)
Insr (Mm01211875_m1)
Lpl (Mm00434764_m1)
Lepr (Mm00440181_m1)
Magel2 (Mm00844026_s1)
mTor (Mm00444968_m1)
Nampt (Mm00451938_m1)
Necdin (Ndn) (Mm02524479_s1)
Nono (Mm01234361_g1)
Npy (Mm03048253_m1)
Nsf (Mm00435390_m1)
Parkin (Mm01323528_m1)
Per2 (Mm00478113_m1)
Per1 (Mm00501813_m1)
Pgc1 alpha (Ppargc1a) (Mm01208835_m1 ())
Pomc (Mm00435874_m1)
Ppar alpha (Ppara) (Mm00440939_m1)
Ppar delta (Ppard) (Mm00803184_m1)
Npas2 (Mm00500848_m1)
Rev-erb alpha (Rev-erba/Nr1d1) (Mm00520711_g1)
Ror alpha (Rora) (Mm01173766_m1)
Sirt1 (Mm01168521_m1)
Sirt3 (Mm00452131_m1)
Sncb (Mm 00504325-m1)
Syn2 (Mm01184324_m1)
Tbp (Mm00446971_m1)
Ucp2 (Mm00627599_m1)

Statistics. Data are presented as means ± SEM. Student's *t* tests were used to compare means for a given parameter (e.g., body mass and length, adiposity, plasma metabolites and hormones, free-running period) between the two genotypes. Two-way analyses of variance (ANOVAs) with repeated measures (RM) were used to compare circadian variations of energy metabolism and food intake and daily rhythms of wheel-running activity. If significant effects ($p < 0.05$) were found between the genotypes and/or between different time-points, pairwise comparisons were performed with post hoc Bonferroni's *t* test (SigmaPlot V13, Systat Software).

For analysis of daily patterns of energy metabolism and feeding, data were fitted to double-peak cosinor regressions (SigmaPlot V13) to take into account the bimodal patterns observed in WT mice. The bimodal regression model was as follows:

$$[y = A + (B \cdot \cos(2 \cdot \pi \cdot (x - C)/24)) + (D \cdot \cos(4 \cdot \pi \cdot (x - E)/24))],$$

where A is the mean level, B the amplitude, C the acrophase of the 24 h rhythm, D and E the amplitude, and the acrophase of the 12 h rhythm, respectively. Daily rhythmicity assessed with bimodal cosinor regressions was considered significant when $p < 0.05$.

For analysis of daily patterns of plasma parameters and gene expression, data were fitted to unimodal cosinor regressions (SigmaPlot V13) as follows:

$$[y = A + (B \cdot \cos(2 \cdot \pi \cdot (x - C)/24))],$$

where A is the mean level (mesor), B the amplitude, and C the acrophase of the 24 h rhythm. Daily rhythmicity was considered significant when $p < 0.05$, and trending for rhythmicity was considered for $0.05 < p < 0.1$. Significant A, B, or C fitted values ± SEM were compared between genotypes with *t* tests to assess effects on mean levels (up- or downregulation), amplitude, and phase-shifts (phase-advances or delays), respectively (SigmaPlot V13).

Results

Altered circadian pattern of metabolism in *Bmal2* KO mice

At 8 months of age, B2KO mice were heavier than WT animals ($t_{(13)} = 2.476$; $p = 0.0278$; *t* test), but not larger ($t_{(13)} = 1.624$; $p = 0.128$; *t* test; Table 1). These changes were associated with marked increased adiposity in the B2KO group ($t_{(13)} = 3.103$; $p = 0.0084$; *t* test). While fasting levels at midday did not differ between the two genotypes ($t_{(13)} = 0.406$; $p = 0.692$; *t* test; Table 1), daily variations of plasma NEFA levels were rhythmic in both fed genotypes and higher in the B2KO group ($t_{(46)} = 2.323$; $p = 0.0246$; Fig. 1*A*). Plasma total cholesterol was not rhythmic in WT mice, but was rhythmic in B2KO mice, and did not differ in mean levels ($t_{(46)} = 1.731$; $p = 0.0901$; Fig. 1*B*). Daily variations of plasma glucose, which were rhythmic in WT mice and not rhythmic in B2KO group, did not differ in mean levels ($t_{(45)} = 0.0288$; $p = 0.977$; Fig. 1*C*). Plasma insulin was not rhythmic in either fed WT and B2KO groups and did not differ in mean levels ($t_{(46)} = 0.464$; $p = 0.645$; Fig. 1*D*). In contrast, fasting plasma insulin at ZT6 was higher in B2KO mice compared with WT littermates ($t_{(13)} = 3.766$; $p = 0.0023$; *t* test), thus suggesting impaired glucose regulation (Table 1). While an oral glucose tolerance test did not detect impaired glucose tolerance, an insulin tolerance test revealed insulin resistance in B2KO mice compared with that in WT control animals (data not shown).

Table 1. Plasma parameters

Parameter	WT	KO *Bmal2*
Body mass (g)	34.9 ± 0.7	39.7 ± 1.6*
Body length (mm)	10.5 ± 0.1	10.3 ± 0.07
Adiposity (% EAT/BM)	2.6 ± 0.2	4.1 ± 0.4**
Plasma glucose (mmol/L)	15.8 ± 1.1	16.9 ± 0.6
Plasma insulin (μg/L)	1.3 ± 0.2	4.0 ± 0.6**
Plasma NEFA (mmol/L)	0.40 ± 0.01	0.38 ± 0.03
Plasma total cholesterol (mmol/L)	4.3 ± 0.2	4.8 ± 0.3

Three-hour fasted WT ($n = 7$) and KO *Bmal2* groups ($n = 7$–8) sampled at midday (ZT6). BM, body mass; EAT, epididymal adipose tissue; NEFA, nonesterified fatty acids.
*$p < 0.05$.
**$p < 0.01$.

During the first day of constant darkness, RER displays a circadian rhythm in both WT and B2KO genotypes ($F_{(4,164)} = 11.909$, $p < 0.0001$, bimodal cosinor for WT; $F_{(4,163)} = 15.406$, $p < 0.0001$, bimodal cosinor for B2KO; main effect of time of day: $F_{(23,276)} = 12.924$, $p < 0.001$, two-way RM ANOVA; Fig. 2*A*). Circadian changes in energy expenditure were present and bimodal in both WT and B2KO genotypes ($F_{(4,163)} = 6.861$, $p < 0.0001$ and $F_{(4,163)} = 4.824$, $p = 0.0011$, respectively; bimodal cosinors; main effect of time of day: $F_{(23,276)} = 8.046$, $p < 0.001$, two-way RM ANOVA). The significant time of day × genotype interaction reveals a propensity for lower night-time energy expenditure in B2KO mice ($F_{(23,276)} = 1.899$, $p = 0.009$, two-way RM ANOVA; Fig. 2*B*).

Altered bimodal pattern of feeding in *Bmal2* KO mice

During the first day of constant darkness, the total amount of food intake per 24 h was similar between both genotypes (4.08 ± 0.24 vs 4.22 ± 0.41 g/day in WT and B2KO, respectively; $t_{(12)} = 0.284$, $p = 0.781$, *t* test). In contrast, the temporal distribution of food intake was different between the two genotypes (time of day × genotype interaction: $F_{(23,276)} = 1.708$, $p = 0.025$, two-way RM ANOVA). More precisely, food intake at dusk was significantly increased in B2KO mice 1 h before WT mice ($t_{(CT11)} = 3.000$; $p = 0.003$; post hoc Bonferroni's *t* test). Second, the dawn peak of feeding in B2KO mice was significantly delayed

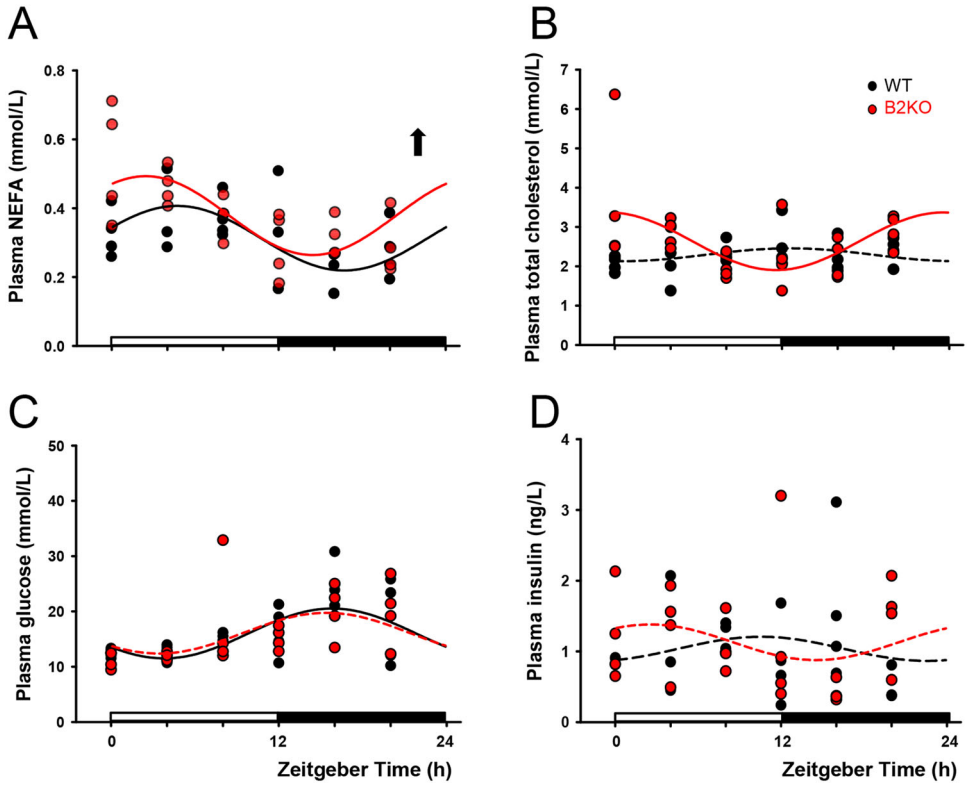

Figure 1. Daily variations of plasma metabolites and insulin of WT mice and mice with deletion of *Bmal2* (B2KO) fed *ad libitum* under light/dark conditions. NEFA, nonesterified fatty acids. Black and red circles represent WT and B2KO mice, respectively. As assessed with cosinor regressions, fitted solid represent significant rhythms, while short dashed lines show nonrhythmic patterns. Black up arrow indicates significant upregulation (*t* test; $p < 0.05$).

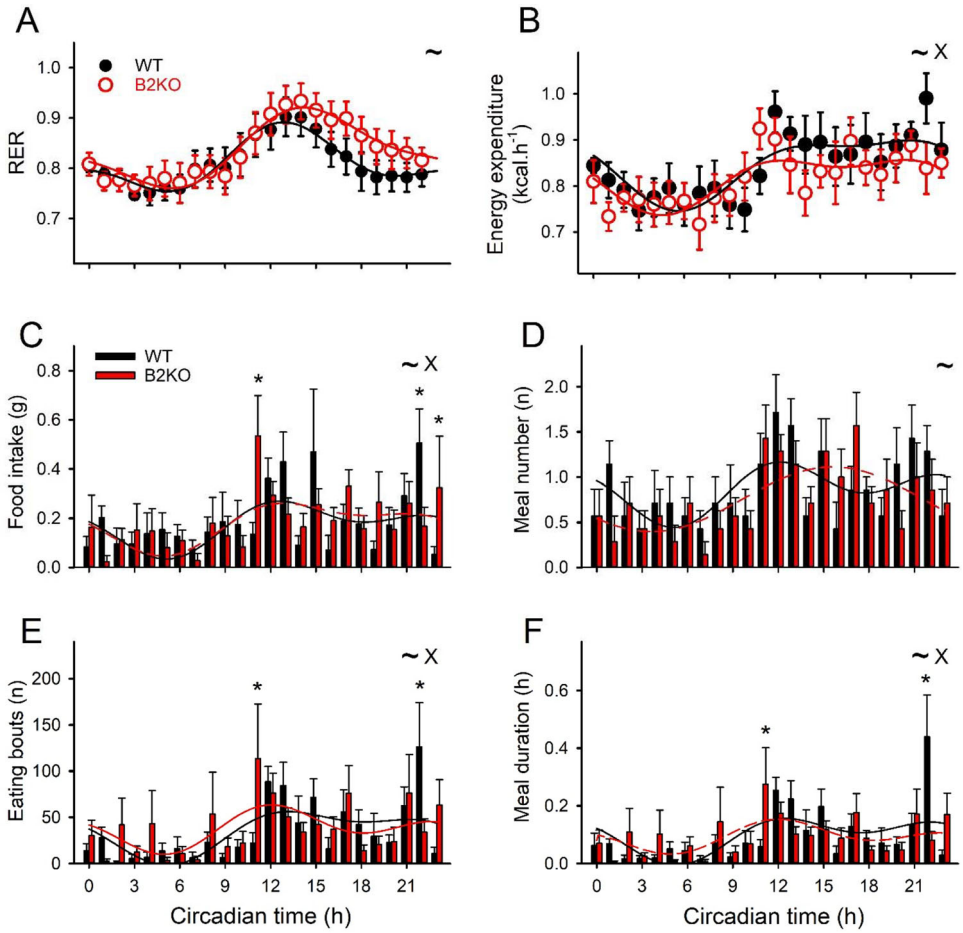

Figure 2. Circadian variations of RER (***A***), energy expenditure (***B***), food intake (***C***), number of meals (***D***), eating bouts (***E***), and meal duration (***F***) in WT (control; black curves and histograms) and mice with deletion of *Bmal2* (B2KO; red curves and histograms) under constant darkness. Data shown on *x*-axis are recorded during the first day of constant darkness and expressed in circadian hours, CT0 and CT12 being projected times of lights on and lights off from the previous light/dark cycle, respectively. RER data for CT23 were discarded due to interferences with calibration process of the calorimetry setup. Fitted solid and dashed lines represent significant and nonsignificant double-peak cosinor regressions, respectively. ∼, significant effect of time of day (2-way RM ANOVA; $p < 0.05$); *X*, significant interaction between genotype and time of day (2-way RM ANOVA, $p < 0.05$); *, intergenotype difference for a given circadian hour (after post hoc Bonferroni's *t* test).

compared with that in WT mice ($t_{(CT22)} = 2.927$, $p = 0.004$ and $t_{(CT23)} = 2.458$, $p = 0.015$, post hoc Bonferroni's *t* tests; Fig. 2*C*). These changes led to a longer eating window in B2KO mice. Furthermore, WT mice displayed a bimodal pattern of food intake, characterized by a dusk peak at the beginning of the active period, a dawn peak at the end of the active period, and a low intake during the resting phase ($F_{(4,163)} = 3.777$, $p = 0.0058$, bimodal cosinor). The circadian pattern of feeding in *Bmal2* KO mice, albeit significant for the 24 h component of cosinor ($F_{(4,163)} = 4.410$; $p = 0.0021$), does not show a significant 12 h bimodal component ($t_{(D)} = 1.899$; $p = 0.059$; *t* test; Fig. 2*C*).

The number of meals across the 24 h were rhythmic in both WT and B2KO mice ($F_{(4,163)} = 2.8019$, $p = 0.0277$ and $F_{(4,163)} = 5.6637$, $p = 0.0003$, cosinor in WT and B2KO, respectively), but the 12 h bimodal component was not significant in B2KO mice ($t_{(D)} = 1.597$; $p = 0.1122$; *t* test; Fig. 2*D*).

In contrast, eating bouts were found rhythmic and bimodal in both genotypes ($F_{(4,163)} = 6.0105$, $p = 0.0002$ and $F_{(4,163)} = 2.4755$, $p = 0.0463$, bimodal cosinor in WT and B2KO, respectively). Furthermore, ANOVA detected significant differences according to time of day (time of day × genotype interaction: $F_{(23,276)} = 1.753$, $p = 0.020$, two-way RM ANOVA).

There was an earlier dusk rise in eating bouts in B2KO compared with that in WT mice at CT11 ($t_{(CT11)} = 3.128$; $p = 0.002$; post hoc Bonferroni's *t* test) while at CT22, the dawn rise in eating bouts was lower in B2KO compared with that in WT mice ($t_{(CT22)} = 3.162$; $p = 0.002$; post hoc Bonferroni's *t* test; Fig. 2*E*).

The temporal distribution of meal duration was different between the two genotypes (time of day × genotype interaction: $F_{(23,276)} = 2.396$, $p < 0.001$, two-way RM ANOVA). Meal duration in B2KO mice was longer at CT11 and shorter at CT22, in comparison with respective values in WT animals ($t_{(CT11)} = 2.992$, $p = 0.003$ and $t_{(CT22)} = 4.953$, $p < 0.001$, post hoc Bonferroni's *t* tests). Meal duration across the 24 h was rhythmic in WT mice ($F_{(4,163)} = 5.4937$; $p = 0.0004$; bimodal cosinor), but not in B2KO mice ($F_{(4,163)} = 2.213$; $p = 0.0698$; bimodal cosinor; Fig. 2*F*).

Bmal2 KO mice have shorter free-running period

In constant darkness, the free-running period of wheel-running activity rhythm was significantly shorter in *Bmal2* KO mice as compared with that in WT controls ($t_{(12)} = 3.514$; $p = 0.0043$; *t* test; Fig. 3).

Clock gene expression in the master clock of *Bmal2* KO mice is not markedly modified

Besides the lack of expression of *Bmal2* and the loss of *Cry1* rhythmicity, no significant change in phase or amplitude was detected in the rhythmic patterns of other clock genes (e.g.,

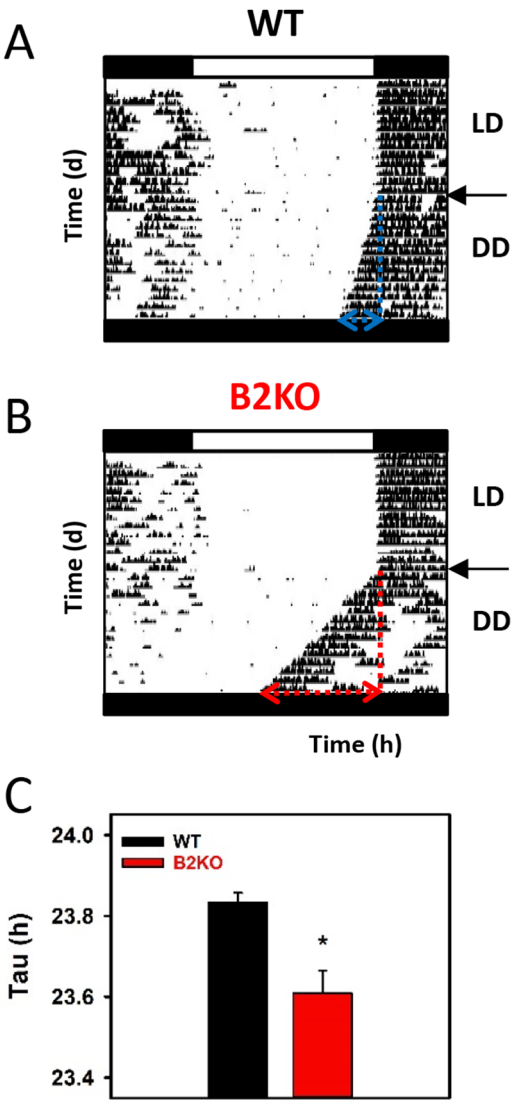

Figure 3. Circadian rhythm of wheel-running activity in WT (control) and mice with deletion of *Bmal2* (B2KO). Representative actograms of WT (***A***) and B2KO (***B***) mice under a light/dark cycle (LD) and then transferred for 2 weeks in constant darkness (DD). Alternations of white and black rectangles on the *x*-axis represent 12 h LD cycles, while fully black rectangles on the *x*-axis represent the whole circadian cycle in DD. ***C***, Mean values of tau (i.e., free-running period) in WT (black histogram) and B2KO mice (red histograms). Note the shorter endogenous period in B2KO mice (*t* test; $p < 0.05$).

Bmal1, *Per2*, *Rev-erbα*, and *Npas2*), in the SCN of B2KO mice. *Clock* expression which is generally considered to be constitutive in the SCN of C57BL6J mice (Zheng et al., 1999; Shearman et al., 2000) showed a trending rhythm in WT SCN, as previously reported by others (Abe et al., 2001). Of note, *Clock* expression was rhythmic in the SCN of B2KO mice in phase with other circadian bHLH-PAS genes (i.e., *Bmal1* and *Npas2*; for statistics, see Fig. 4, Extended Data Fig. 4-1, and Extended Data Table 4-1).

Metabolic gene expression loses daily rhythmicity in the master clock of *Bmal2* KO mice

In contrast, rhythmic genes involved in intracellular metabolism, such as *Ucp2* and *Lpl*, and *Nampt* (trending rhythmic expression), displayed arrhythmic patterns of expression in the SCN of B2KO mice. Regarding *Pparα* and leptin receptor (*lepR*), their rhythmic expression was phase-delayed by >3 h in the SCN of B2KO individuals, as compared with respective expression profiles in WT mice. Furthermore, expression of *Nsf* coding for vesicle-fusing ATPase, a protein involved in synapse activity, may be used as a marker of neuronal activity, while increased expression of *Gfap* coding glial fibrillary acidic protein may be used as an index of astroglial activation. Expression of both *Nsf* and *Gfap* displayed trending rhythmicity in the WT SCN but showed arrhythmicity in the SCN of B2KO mice. In addition, daily levels of both *Sirt3* and *Necdin* (*Ndn*) were upregulated in the SCN of B2KO mice, in comparison with those in WT littermates (for statistics, see Fig. 4, Extended Data Fig. 4-1, and Extended Data Table 4-1).

Impaired meal anticipation in *Bmal2* KO mice

To test whether *Bmal2* deletion modifies behavioral anticipation to meal time, both WT and B2KO mice were challenged with 6 h restricted feeding, food being available from midday to dark onset. The level of daily (i.e., total) wheel-running activity under a light/dark cycle was not significantly different in B2KO mice fed *ad libitum* as compared with WT animals (7,675 ± 1,326 vs 10,680 ± 1,416 wheel revolutions/24 h, respectively; $t_{(13)} = 1.548$, $p = 0.146$, *t* test; see daily patterns in Fig. 5). The level of total wheel-running activity during restricted feeding was not significantly different between B2KO and WT mice (9,100 ± 1,559 vs 9,170 ± 1,666 wheel revolutions/24 h, respectively; $t_{(13)} = 0.0310$, $p = 0.976$, *t* test; see daily pattern in Fig. 5*A–D*).

In contrast, two-way RM ANOVA detected a significant main effect of time of day ($F_{(23,299)} = 34.522$; $p < 0.001$) and a significant time of day × genotype interaction ($F_{(23,299)} = 1.839$; $p = 0.012$). After a few days of restricted feeding, WT mice expressed an increase of wheel-running activity 1–2 h before food access, defining food-anticipatory activity (Mistlberger, 2011; Delezie et al., 2016). B2KO mice did not show such an anticipatory bout of activity ($t_{(ZT05)} = 3.227$; $p = 0.001$; post hoc Bonferroni's *t* test; Fig. 5*B*,*D*). Furthermore, while the levels of nocturnal activity during restricted feeding were comparable in both genotypes during early and late night, there was a significant increase of wheel-running activity around midnight in B2KO individuals compared with that in WT mice ($t_{(ZT16)} = 3.477$, $p < 0.001$ and $t_{(ZT17)} = 2.756$, $p = 0.006$, post hoc Bonferroni's *t* tests; see Fig. 5*D*).

Because light during daytime may exert inhibitory effects on voluntary exercise, including food-anticipatory activity (Patton et al., 2013), such masking effects of light may explain why *Bmal2* KO mice display weak anticipation to daytime food access. To test this hypothesis, we transferred all mice to a skeleton photoperiod for 2 weeks. During the first day(s) of this new lighting condition, food-anticipatory activity in B2KO mice does not appear to be stronger than under previous light/dark conditions. However, in sharp contrast to WT mice, exposure to skeleton photoperiod led to a temporal disorganization of locomotor activity rhythm, with in most cases a rapid drift of the nocturnal pattern of activity toward and beyond the time of food access. This drift precludes us from quantifying food-anticipatory activity in B2KO mice with accuracy under skeleton photoperiod (Extended Data Fig. 5-1).

In animals fed *ad libitum* housed constant darkness, but after being faced with restricted feeding, the free-running period was still found shorter in B2KO animals compared with that in WT mice (23.10 ± 0.12 vs 23.58 ± 0.04 h, $n = 6$ and 7, respectively; $t_{(11)} = 4.105$, $p = 0.00175$, *t* test; see actograms in Extended Data Fig. 5-1). Incidentally, one B2KO mouse displayed an arrhythmic

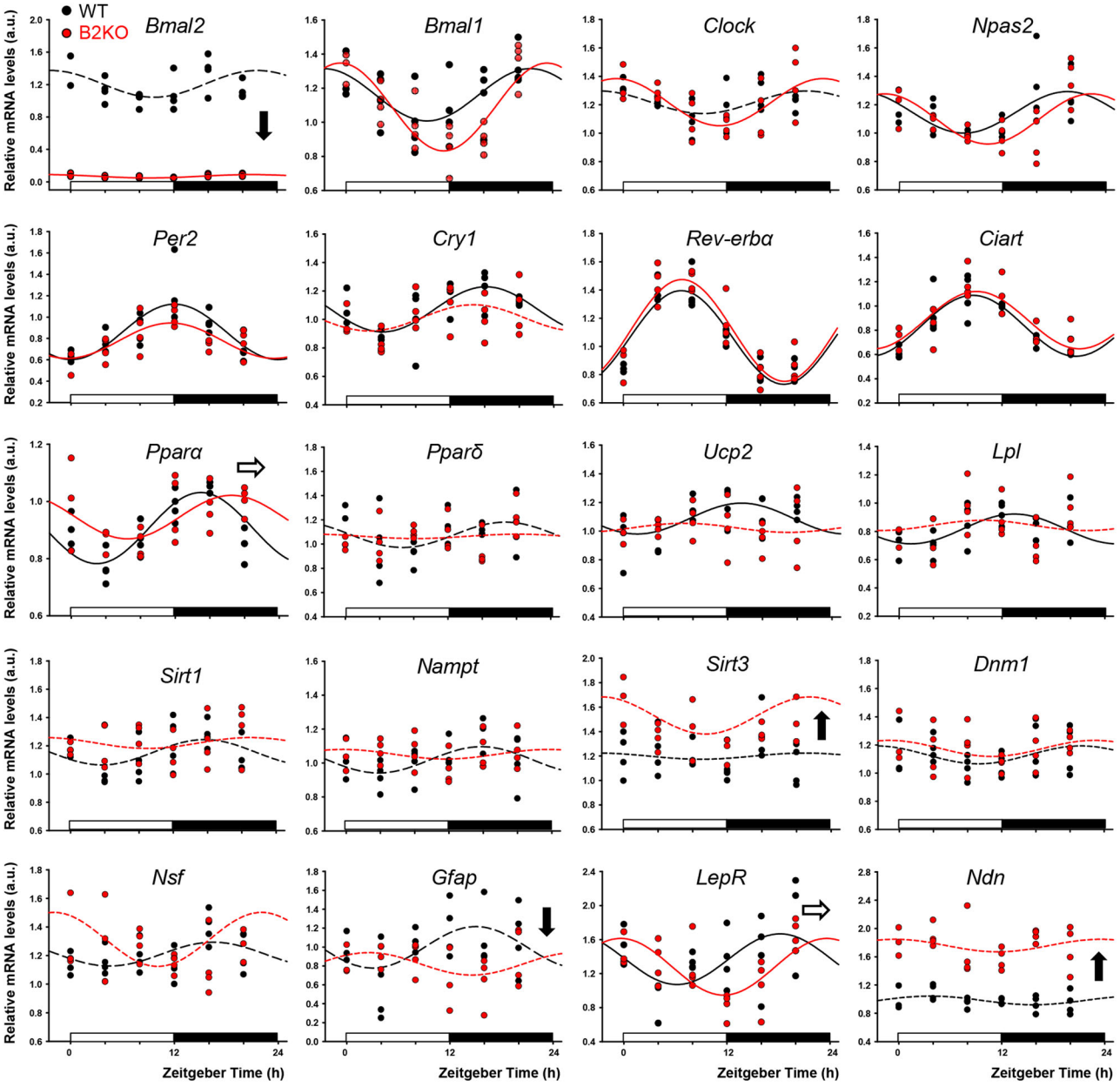

Figure 4. Daily expression of clock and metabolic genes in the suprachiasmatic nuclei of the hypothalamus of WT mice and mice with deletion of *Bmal2* (B2KO) under light/dark conditions. Black and red circles represent WT and B2KO mice, respectively. As assessed with cosinor regressions, fitted solid and long dashed lines represent significant and trending rhythms, respectively, while short dashed lines show nonrhythmic patterns. Black down and up arrows indicate significant down- and upregulation, respectively (*t* test; $p < 0.05$). Horizontal white arrows indicate significant phase-shifts (*t* test; $p < 0.05$). a.u., arbitrary unit. Statistical analyses of cosinor regressions are shown in Extended Data Table 4-1. Heatmap of gene expression in the SCN is shown in Extended Data Figure 4-1.

circadian pattern of locomotor activity (see panel bottom left right, Extended Data Fig. 5-1). Compared with the initial period measurement, note that the shortening of the circadian period in B2KO mice was twofold more pronounced than that in WT animals (delta of 0.46 ± 0.08 vs 0.25 ± 0.06 h, respectively; $t_{(11)} = 2.168$; $p = 0.0530$; *t* test).

Mild alterations of clock gene expression in the MBH of *Bmal2* KO mice

In keeping with results in the SCN clockwork, the rhythmic patterns of clock genes in the MBH of B2KO mice were close to those of WT mice. As in the SCN, while they only tended to be rhythmic in the WT MBH, *Clock* levels displayed a rhythmic expression in the MBH of B2KO mice. In addition, mean levels of *Rev-erbα* were higher in the MBH of B2KO mice as compared with WT individuals (for statistics, see Fig. 6, Extended Data Fig. 6-1, and Extended Data Table 6-1).

Altered expression of metabolic and orexigenic genes in the MBH of *Bmal2* KO mice

Several metabolic genes showed arrhythmic patterns of expression in both WT and B2KO mice. Nevertheless, expression of *Lpl* and mitochondrial genes (*Sirt3* and *Dnm1*) in the MBH displayed trending rhythms in control mice and were arrhythmic in B2KO mice. Furthermore, it is noteworthy that expression of three genes coding orexigenic peptides (i.e., *Npy*, *AgRP*, and

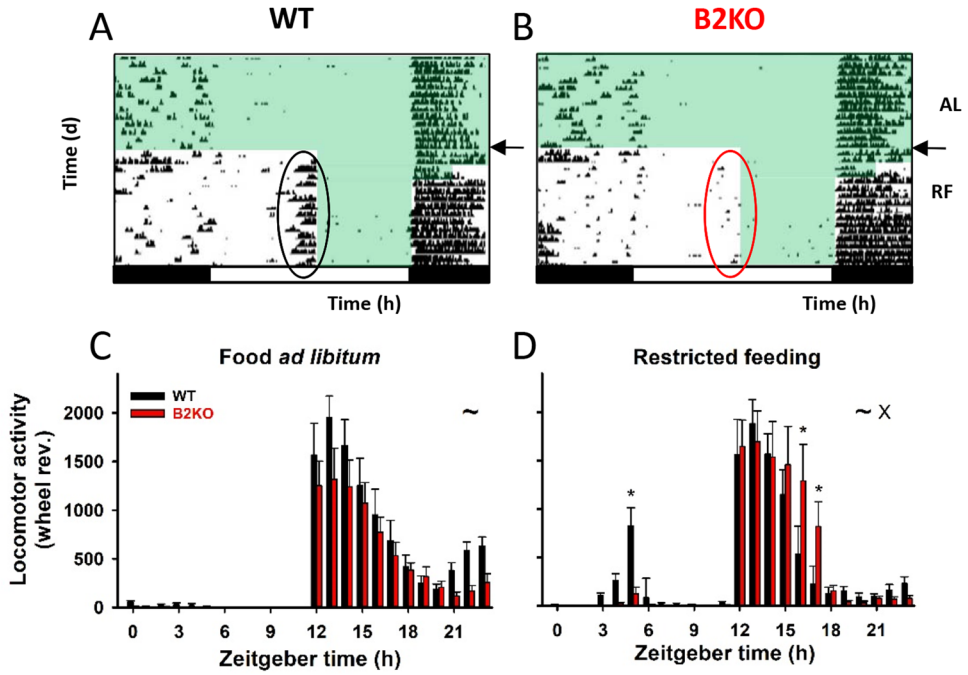

Figure 5. Representative actograms of WT mice (panel ***A***) and mice with deletion of *Bmal2* (B2KO; panel ***B***) mice under a light/dark cycle and challenged with restricted feeding schedule limited progressively to 6 h per day from midday to lights off. Green boxes denote timing of food availability. Note that food-anticipatory activity expressed by the WT mouse is hardly visible in the B2KO mouse. Daily activity profiles in both genotypes fed with food *ad libitum* (***C***) and restricted feeding schedule (***D***). Data shown on *x*-axis are expressed in Zeitgeber hours, ZT0 and ZT12 being times of lights on and lights off, respectively. ∼, significant effect of time of day (2-way RM ANOVA, $p < 0.05$); *X*, significant interaction between genotype and time of day (2-way RM ANOVA, $p < 0.05$); *, intergenotype difference for a given circadian hour (after post hoc Bonferroni's *t* test). In contrast to the clear behavioral anticipation of food access timing in WT mice, note the lack of salient anticipation of food availability in B2KO mice. The actograms of WT and B2KO mice challenged with restricted feeding under a light/dark cycle, followed by skeleton photoperiod and constant darkness are shown in Extended Data Figure 5-1.

Hcrt/Orexin) was downregulated in B2KO mice, while expression of anorexigenic genes (*Pomc* and *Cart*) was not significantly modified (Fig. 6, Extended Data Fig. 6-1, and Extended Data Table 6-1). Unlike for the SCN, *Gfap* expression in the MBH displayed a trending rhythmicity in the WT animals and showed a significant rhythmicity in B2KO mice. Also, daily levels of *Ndn* were upregulated in the MBH of B2KO mice, compared with those in WT animals (for statistics, see Fig. 6, Extended Data Fig. 6-1, and Extended Data Table 6-1).

Discussion

The present data reveal that a global deletion of *Bmal2* leads to metabolic and circadian alterations, including mild obesity, altered circadian pattern of energy metabolism and feeding, markedly reduced food anticipation, shorter free-running period, and loss of rhythmicity of metabolic genes in brain clocks. Together, these findings fit with the predicted function of *Bmal2* in circadian rhythm regulation and highlight its widespread involvement in brain control of metabolic physiology and behavior.

The shorter free-running period in *Bmal2* KO mice indicates that *Bmal2* is a clock gene involved in function of the SCN clock. Without BMAL2, the speed of the master clock is thus accelerated. Of note, constitutive expression of BMAL2 leads to an opposite change (i.e., lengthening) of the circadian period (S. Shi et al., 2010). Furthermore, diet-induced obesity also leads to a lengthened period of the master clock (Kohsaka et al., 2007; Mendoza et al., 2008), suggesting that the shorter period in obesity-prone B2KO mice is not a consequence of increased adiposity.

Because the nocturnal pattern of locomotor activity is controlled by the SCN clock, the continuous drift of nocturnal pattern under skeleton photoperiod combined with daytime restricted feeding in B2KO mice suggests that the skeleton photoperiod does not provide photic cues strong enough to entrain the master clock of B2KO mice that is neither synchronized to meal time. Accordingly, the drift of locomotor activity rhythm in B2KO mice under skeleton photoperiod may reflect either a weak SCN clock, a poor synchronization to light, or a combination of both.

Besides the arrhythmicity of one animal under these conditions, the 0.5 h shortening of the circadian period in *Bmal2* KO mice over the experiment indicates stronger aftereffects of restricted feeding and/or skeleton photoperiod on the master clock of B2KO mice, as compared with that in WT mice. In addition, the higher interindividual variability of the circadian period in *Bmal2* KO animals suggests that BMAL2 contributes to the precision of the circadian time-keeping system, as previously proposed for another clock protein, REV-ERBα (Preitner et al., 2002).

The apparent weak clockwork in B2KO mice, however, does not translate into clear alterations of daily profiles of clock gene expression in the master clock. Deletion of *Bmal2* may actually affect the functional interactions between metabolic intracellular pathways and the molecular clockwork. It is worth noting that a number of intracellular regulators lost daily rhythmicity in the SCN of these mice. They include, on the one hand, genes (e.g., *Ucp2* and eventually *Nampt*) coding for proteins participating notably in the cellular protection from reactive oxygen species (Arsenijevic et al., 2000; de Guia et al., 2020; Singh and Ubaid, 2020) and, on the other hand, genes (i.e., *Lpl*) coding

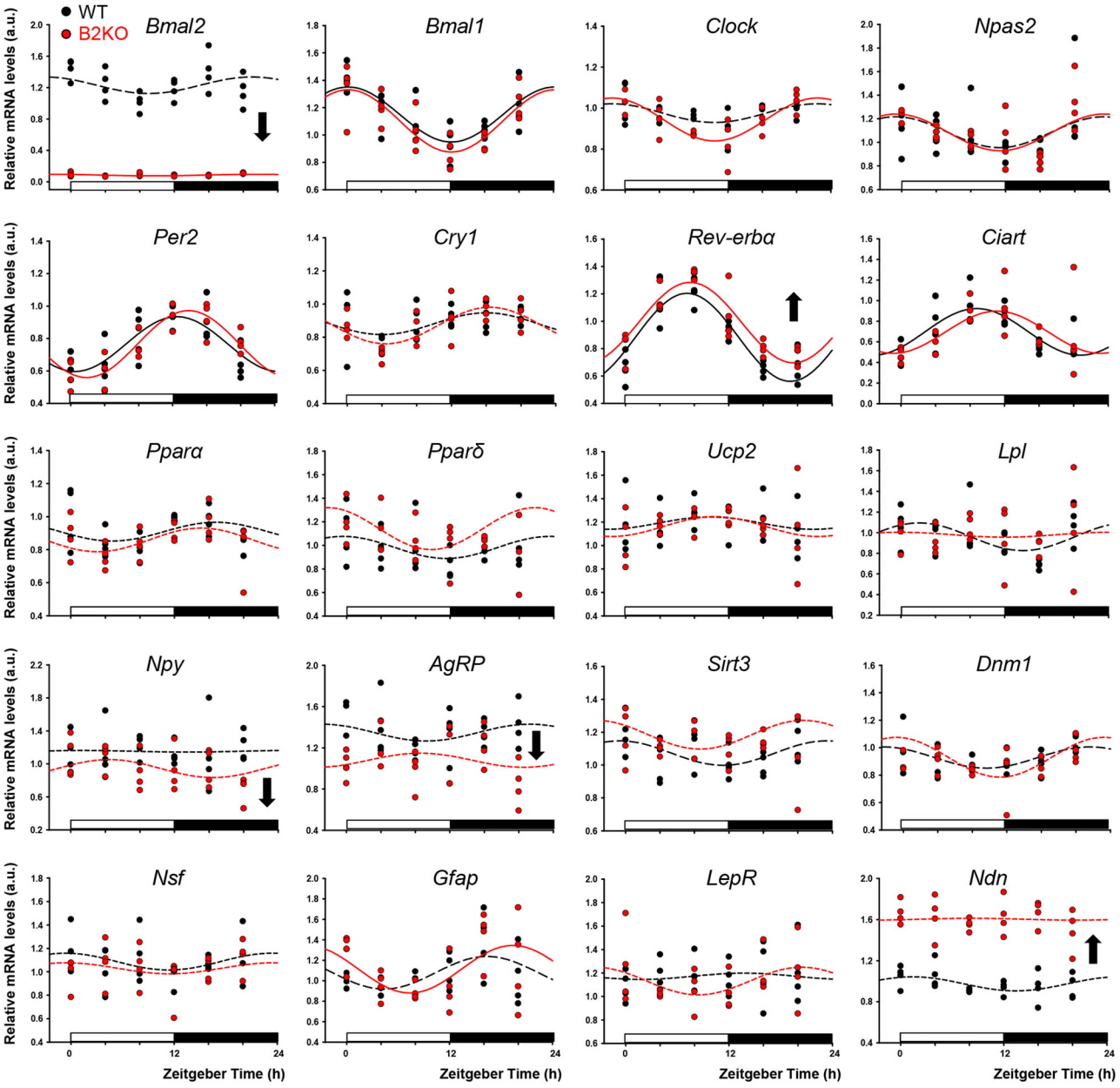

Figure 6. Daily expression of clock, orexigenic, anorexigenic, and metabolic genes in the MBH of WT mice and mice with deletion of *Bmal2* (B2KO) under light/dark conditions. Black and red circles represent WT and B2KO mice, respectively. As assessed with cosinor regressions, fitted solid and long dashed lines represent significant and trending rhythms, respectively, while short dashed lines show nonrhythmic patterns. Black down and up arrows indicate significant down- and upregulation, respectively (*t* test; $p < 0.05$). a.u., arbitrary unit. Statistical analyses of cosinor regressions are shown in Extended Data Table 6-1. Heatmap of gene expression in the MBH is shown in Extended Data Figure 6-1.

for regulators of brain lipid metabolism (Laperrousaz et al., 2017). A limitation of this work is that only mRNA abundance has been studied, which provides no information on protein level or activity. Other omic techniques such as proteomics and metabolomics are required to investigate these issues further. Nevertheless, the present findings illustrate a weak clockwork of the SCN in the absence of *Bmal2* and suggest also that BMAL2 in the master clock is an important regulator of the daily rhythmicity of intracellular metabolism.

When challenged with timed restricted feeding, mice lacking *Bmal2* exhibit strongly diminished food anticipation, suggesting that this gene is a component of the food clock. Dampened food anticipation under a light/dark cycle was also observed in skeleton photoperiod, although such photoperiodic conditions combined with restricted feeding led to unexpected temporal disorganization of daily behavior in a number of *Bmal2* KO mice. In some food-restricted B2KO mice exposed to a skeleton photoperiod, a drift of the nocturnal pattern took a few days to occur. In these mice, the reduced behavioral anticipation of daily food access persisted under a skeleton photoperiod. This confirms that the impairment of daytime food anticipation in B2KO mice is not due to an increased masking effect of light that would have inhibited the expression of food-anticipatory activity (Patton et al., 2013).

Whether clock genes participate or not in the molecular mechanisms of the food clock has been the subject of debate over the last decade. Depending on the mutated/deleted gene, on the type of deletion, and even for the same genotype tested

by different laboratories, food anticipation in mice with genetically impaired clocks is found to be altered or normal (Challet et al., 2009; Storch and Weitz, 2009; Mieda and Sakurai, 2011; Takasu et al., 2012; Delezie et al., 2016; Pendergast and Yamazaki, 2018). In agreement with previous data supporting an involvement of brain BMAL1 in food anticipation (Mieda and Sakurai, 2011), the present data indicate that BMAL2 is another clock cog of the food clock. Brain regulation of *Bmal2* has been hardly investigated. Nevertheless, *Bmal2* expression in the central nervous system is considered to be restricted to neurons (Drutel et al., 1999). Accordingly, this feature raises the possibility that the observed changes in gene expression occur in neurons, eventually also in the peripheral nervous system. If correct, this assumption suggests that some of the observed effects may be due to altered regulation of peripheral physiology that would feedback to the brain. If confirmed, the neuronal expression of *Bmal2* also suggests that the food clock involves BMAL2 in neuronal clocks. In line with the SCN, daily profiles of clock genes in the MBH were close between B2KO and WT mice. In addition, daily expression of *Lpl* in the MBH was respectively rhythmic and arrhythmic in WT and B2KO, as also found in the SCN clock. These close results in the master clock and a set of secondary hypothalamic clocks support the notion that BMAL2 may be a functional link between circadian clocks and rhythmicity of some metabolic pathways. Among the strongest consequence of *Bmal2* deletion is the overexpression of *Necdin* (*Ndn*) in the hypothalamus. NDN is a transcriptional factor expressed in postmitotic neurons that participates in many intracellular pathways, such as cellular metabolism, transcriptional regulation, and signal transduction (Yoshikawa, 2021). Interestingly, NDN binds to BMAL2 to repress its transcriptional activation (Friedman and Fan, 2007). The upregulated levels of *Ndn* in B2KO mice indicate in turn that BMAL2 downregulates *Ndn* expression. In the same line, expression of *Sirt3*, a mitochondrial sirtuin playing a major role in cellular homeostasis and aging (van de Ven et al., 2017), is markedly increased in the SCN of B2KO animals, suggesting that BMAL2 represses *Sirt3* transcription.

Even if expression of two genes coding orexigenic peptides (i.e., *Npy* and *AgRP*) was downregulated in B2KO mice, the homeostatic regulation of energy intake does not clearly rely on *Bmal2* because the daily amount of food intake was similar between age- and sex-matched B2KO and WT mice. The daily feeding/fasting cycle is thought to be controlled by a network of cerebral circadian clocks in the hypothalamus and brainstem linked to the light-entrainable master clock and to peripheral organs that harbor food-entrainable clocks and send meal-related temporal and metabolic cues to the brain (Challet, 2019). Accordingly, there was a nocturnal bimodal pattern of feeding in WT mice, mostly characterized by dawn and dusk peaks of food intake, larger number of meals, and eating bouts. In contrast, *Bmal2* KO mice did not display significant bimodality in circadian rhythms of food intake and meal numbers, highlighting impaired temporal control of eating on a 24 h scale. It is noteworthy that a number of mice with defective circadian clocks display dampening, if not arrhythmicity, in daily or circadian pattern of feeding, including *Per1/2* (Adamovich et al., 2014), *Cry1/Cry2* (Kettner et al., 2015), and *Rev-erbα* KO mice (Sen et al., 2018). The dusk peak being considered to involve the SCN in nocturnal rodents (Strubbe and van Dijk, 2002), its temporal disturbances in B2KO mice could thus result from an impaired master clock. On the other hand, the dawn peak may imply the food clock (Challet, 2019). The earlier dawn peak in B2KO mice may be related to mismatched network of food-entrainable processes, as supported with their impaired anticipation of food availability.

BMAL2 has been proposed to inhibit adipogenesis (Mandl et al., 2022), which is in line with the increased adiposity and NEFA levels we found in B2KO mice. Other regulatory factors may contribute to the obese phenotype in these mice. During the resting (daytime) period, B2KO and WT mice express close values of RER and energy expenditure, suggesting that the two groups of mice similarly utilize lipids and display matching basal metabolic rate. Despite comparable levels of locomotor activity and food intake at night, a trend to lower energy expenditure during their active phase suggests that *Bmal2* KO mice may accumulate more energy stores than WT mice. This observation fits with increased adiposity in B2KO mice, although other factors may also be involved. In addition, specific deletion of *Bmal2* in cerebral clocks will be useful to rule out phenotypic alterations that may result from its peripheral deletion in B2KO mice.

Altogether, the present findings at behavioral, physiological, and molecular levels indicate that *Bmal2* is a clock gene important for the brain regulation of circadian behavior and metabolic health.

References

Abe H, Honma S, Namihira M, Masubuchi S, Ikeda M, Ebihara S, Honma K (2001) Clock gene expressions in the suprachiasmatic nucleus and other areas of the brain during rhythm splitting in CS mice. Brain Res Mol Brain Res 87:92–99.

Adamovich Y, Rousso-Noori L, Zwighaft Z, Neufeld-Cohen A, Golik M, Kraut-Cohen J, Wang M, Han X, Asher G (2014) Circadian clocks and feeding time regulate the oscillations and levels of hepatic triglycerides. Cell Metab 19:319–330.

Arble DM, et al. (2015) Impact of sleep and circadian disruption on energy balance and diabetes: a summary of workshop discussions. Sleep 38: 1849–1860.

Arsenijevic D, et al. (2000) Disruption of the uncoupling protein-2 gene in mice reveals a role in immunity and reactive oxygen species production. Nat Genet 26:435–439.

Berthoud HR, Seeley RJ, Roberts SB (2021) Physiology of energy intake in the weight-reduced state. Obesity 29:S25–S30.

Challet E (2019) The circadian regulation of food intake. Nat Rev Endocrinol 15:393–405.

Challet E, Mendoza J, Dardente H, Pevet P (2009) Neurogenetics of food anticipation. Eur J Neurosci 30:1676–1687.

Costa-Urrutia P, Colistro V, Jimenez-Osorio AS, Cardenas-Hernandez H, Solares-Tlapechco J, Ramirez-Alcantara M, Granados J, Ascencio-Montiel IJ, Rodriguez-Arellano ME (2019) Genome-wide association study of body mass index and body fat in Mexican-Mestizo children. Genes 10:945.

Dardente H, Fortier EE, Martineau V, Cermakian N (2007) Cryptochromes impair phosphorylation of transcriptional activators in the clock: a general mechanism for circadian repression. Biochem J 402:525–536.

de Guia RM, et al. (2020) Fasting- and ghrelin-induced food intake is regulated by NAMPT in the hypothalamus. Acta Physiol 228:e13437.

Delezie J, Dumont S, Sandu C, Reibel S, Pevet P, Challet E (2016) Rev-erbalpha in the brain is essential for circadian food entrainment. Sci Rep 6:29386.

Drutel G, Heron A, Kathmann M, Gros C, Mace S, Plotkine M, Schwartz JC, Arrang JM (1999) ARNT2, a transcription factor for brain neuron survival? Eur J Neurosci 11:1545–1553.

Friedman ER, Fan CM (2007) Separate necdin domains bind ARNT2 and HIF1alpha and repress transcription. Biochem Biophys Res Commun 363:113–118.

Guilding C, Hughes AT, Brown TM, Namvar S, Piggins HD (2009) A riot of rhythms: neuronal and glial circadian oscillators in the mediobasal hypothalamus. Mol Brain 2:28.

He CX, Avner P, Boitard C, Rogner UC (2010a) Downregulation of the circadian rhythm related gene Arntl2 suppresses diabetes protection in

Idd6 NOD.C3H congenic mice. Clin Exp Pharmacol Physiol 37:1154–1158.
He CX, Prevot N, Boitard C, Avner P, Rogner UC (2010b) Inhibition of type 1 diabetes by upregulation of the circadian rhythm-related aryl hydrocarbon receptor nuclear translocator-like 2. Immunogenetics 62:585–592.
Hogenesch JB, Gu YZ, Moran SM, Shimomura K, Radcliffe LA, Takahashi JS, Bradfield CA (2000) The basic helix-loop-helix-PAS protein MOP9 is a brain-specific heterodimeric partner of circadian and hypoxia factors. J Neurosci 20:RC83.
Hung MS, Avner P, Rogner UC (2006) Identification of the transcription factor ARNTL2 as a candidate gene for the type 1 diabetes locus Idd6. Hum Mol Genet 15:2732–2742.
Ikeda M, Yu W, Hirai M, Ebisawa T, Honma S, Yoshimura K, Honma KI, Nomura M (2000) cDNA cloning of a novel bHLH-PAS transcription factor superfamily gene, BMAL2: its mRNA expression, subcellular distribution, and chromosomal localization. Biochem Biophys Res Commun 275:493–502.
Kettner NM, Mayo SA, Hua J, Lee C, Moore DD, Fu L (2015) Circadian dysfunction induces leptin resistance in mice. Cell Metab 22:448–459.
Kohsaka A, Laposky AD, Ramsey KM, Estrada C, Joshu C, Kobayashi Y, Turek FW, Bass J (2007) High-fat diet disrupts behavioral and molecular circadian rhythms in mice. Cell Metab 6:414–421.
Laperrousaz E, et al. (2017) Lipoprotein lipase in hypothalamus is a key regulator of body weight gain and glucose homeostasis in mice. Diabetologia 60:1314–1324.
Lebailly B, Boitard C, Rogner UC (2015) Circadian rhythm-related genes: implication in autoimmunity and type 1 diabetes. Diabetes Obes Metab 17:134–138.
Lebailly B, Langa F, Boitard C, Avner P, Rogner UC (2017) The circadian gene Arntl2 on distal mouse chromosome 6 controls thymocyte apoptosis. Mamm Genome 28:1–12.
Mandl M, et al. (2022) The circadian transcription factor ARNTL2 is regulated by weight-loss interventions in human white adipose tissue and inhibits adipogenesis. Cell Death Discov 8:443.
Mendoza J, Pevet P, Challet E (2008) High-fat feeding alters the clock synchronization to light. J Physiol 586:5901–5910.
Mieda M, Sakurai T (2011) Bmal1 in the nervous system is essential for normal adaptation of circadian locomotor activity and food intake to periodic feeding. J Neurosci 31:15391–15396.
Mistlberger RE (2011) Neurobiology of food anticipatory circadian rhythms. Physiol Behav 104:535–545.
Mohawk JA, Green CB, Takahashi JS (2012) Central and peripheral circadian clocks in mammals. Annu Rev Neurosci 35:445–462.
Okano T, Sasaki M, Fukada Y (2001) Cloning of mouse BMAL2 and its daily expression profile in the suprachiasmatic nucleus: a remarkable acceleration of Bmal2 sequence divergence after Bmal gene duplication. Neurosci Lett 300:111–114.
Olkkonen J, Kouri VP, Kuusela E, Ainola M, Nordstrom D, Eklund KK, Mandelin J (2017) DEC2 blocks the effect of the ARNTL2/NPAS2 dimer on the expression of PER3 and DBP. J Circadian Rhythms 15:6.
Patton DF, Parfyonov M, Gourmelen S, Opiol H, Pavlovski I, Marchant EG, Challet E, Mistlberger RE (2013) Photic and pineal modulation of food anticipatory circadian activity rhythms in rodents. PLoS One 8:e81588.
Paxinos G, Franklin KB (2001) *The mouse brain in stereotaxic coordinates*. San Diego, CA: Academic Press.
Pendergast JS, Yamazaki S (2018) The mysterious food-entrainable oscillator: insights from mutant and engineered mouse models. J Biol Rhythms 33:458–474.
Preitner N, Damiola F, Lopez-Molina L, Zakany J, Duboule D, Albrecht U, Schibler U (2002) The orphan nuclear receptor REV-ERBalpha controls circadian transcription within the positive limb of the mammalian circadian oscillator. Cell 110:251–260.
Salgado-Delgado R, Angeles-Castellanos M, Saderi N, Buijs RM, Escobar C (2010) Food intake during the normal activity phase prevents obesity and circadian desynchrony in a rat model of night work. Endocrinology 151:1019–1029.
Sasaki M, Yoshitane H, Du NH, Okano T, Fukada Y (2009) Preferential inhibition of BMAL2-CLOCK activity by PER2 reemphasizes its negative role and a positive role of BMAL2 in the circadian transcription. J Biol Chem 284:25149–25159.
Scheer FA, Hilton MF, Mantzoros CS, Shea SA (2009) Adverse metabolic and cardiovascular consequences of circadian misalignment. Proc Natl Acad Sci U S A 106:4453–4458.
Schoenhard JA, Eren M, Johnson CH, Vaughan DE (2002) Alternative splicing yields novel BMAL2 variants: tissue distribution and functional characterization. Am J Physiol Cell Physiol 283:C103–C114.
Sen S, Dumont S, Sage-Ciocca D, Reibel S, de Goede P, Kalsbeek A, Challet E (2018) Expression of the clock gene Rev-erbalpha in the brain controls the circadian organisation of food intake and locomotor activity, but not daily variations of energy metabolism. J Neuroendocrinol 30:e12557.
Shearman LP, et al. (2000) Interacting molecular loops in the mammalian circadian clock. Science 288:1013–1019.
Shi S, Hida A, McGuinness OP, Wasserman DH, Yamazaki S, Johnson CH (2010) Circadian clock gene Bmal1 is not essential; functional replacement with its paralog, Bmal2. Curr Biol 20:316–321.
Shi SQ, Ansari TS, McGuinness OP, Wasserman DH, Johnson CH (2013) Circadian disruption leads to insulin resistance and obesity. Curr Biol 23:372–381.
Singh V, Ubaid S (2020) Role of silent information regulator 1 (SIRT1) in regulating oxidative stress and inflammation. Inflammation 43:1589–1598.
Storch KF, Weitz CJ (2009) Daily rhythms of food-anticipatory behavioral activity do not require the known circadian clock. Proc Natl Acad Sci U S A 106:6808–6813.
Strubbe JH, van Dijk G (2002) The temporal organization of ingestive behaviour and its interaction with regulation of energy balance. Neurosci Biobehav Rev 26:485–498.
Takasu NN, Kurosawa G, Tokuda IT, Mochizuki A, Todo T, Nakamura W (2012) Circadian regulation of food-anticipatory activity in molecular clock-deficient mice. PLoS One 7:e48892.
van de Ven RAH, Santos D, Haigis MC (2017) Mitochondrial sirtuins and molecular mechanisms of aging. Trends Mol Med 23:320–331.
Yamaguchi M, et al. (2015) Association between brain-muscle-ARNT-like protein-2 (BMAL2) gene polymorphism and type 2 diabetes mellitus in obese Japanese individuals: a cross-sectional analysis of the Japan multi-institutional collaborative cohort study. Diabetes Res Clin Pract 110:301–308.
Yoshikawa K (2021) Necdin: a purposive integrator of molecular interaction networks for mammalian neuron vitality. Genes Cells 26:641–683.
Zheng B, Larkin DW, Albrecht U, Sun ZS, Sage M, Eichele G, Lee CC, Bradley A (1999) The mPer2 gene encodes a functional component of the mammalian circadian clock. Nature 400:169–173.